Polymer solutions: from hard monomers to soft polymers

Jean-Pierre Hansen, Chris I Addison and Ard A Louis

Department of Chemistry, University of Cambridge, Lensfield Road, Cambridge CB2 1EW, UK

Abstract
A coarse-graining strategy for dilute and semi-dilute solutions of interacting polymers, and of colloid–polymer mixtures, is briefly described. Monomer degrees of freedom are traced out to derive an effective, state-dependent pair potential between the polymer centres of mass. The cross-over between good and poor solvent conditions is discussed within a scaling analysis. The method is extended to block copolymers represented as 'necklaces' of soft 'blobs', and its success is illustrated here in the case of a symmetric diblock copolymer which exhibits microphase separation.

1. Introduction: a coarse-graining strategy

The present paper summarizes a collective effort by the Cambridge group and others to bridge the 'cultural divide' between statistical mechanics of polymer solutions and melts on the one hand and of 'simple liquids' on the other. While the former is dominated by field-theoretic methods and scaling concepts pioneered by S F Edwards and P G de Gennes, the description of simple liquids, which lack the scale invariance of polymers, requires a more atomistic approach. To bridge the gap we have developed a systematic coarse-graining strategy first suggested by Flory and Krigbaum [1], whereby individual monomer degrees of freedom are traced out for fixed centre-of-mass (CM) positions of the polymer coils, thus defining an effective interaction between the CMs. Consider a system of N identical polymer, each consisting of M monomers (or segments) at positions $\vec{r}_{i\alpha}$ ($1 \leqslant i \leqslant N; 1 \leqslant \alpha \leqslant M$). If $H(\{\vec{r}_{i\alpha}\})$ is the interaction Hamiltonian of the system, the probability distribution of the N CMs at positions $\vec{R}_i$ is

$$P_N(\{\vec{R}_i\}) = \frac{1}{Q_N} \int e^{-\beta H(\{\vec{r}_{i\alpha}\})} \prod_{i=1}^{N} \delta\left(\vec{R}_i - \frac{1}{M}\sum_{\alpha} \vec{r}_{i\alpha}\right) \prod_{i=1}^{N}\prod_{\alpha=1}^{M} d\vec{r}_{i\alpha} \qquad (1)$$

$$= \frac{e^{-\beta V_{\text{eff}}(\{\vec{R}_i\})}}{\int e^{-\beta V_{\text{eff}}(\{\vec{R}_i\})} \prod_{i=1}^{N} d\vec{R}_i} \qquad (2)$$

where $\beta = \frac{1}{k_B T}$, Q_N is the partition function for the $N \times M$ monomers, and the total effective interaction energy of the N CMs is rigorously defined by

$$V_{\text{eff}}(\{\vec{R}_i\}) = -k_B T \ln[C \times P_N(\{\vec{R}_i\})]. \qquad (3)$$

This effective energy is a free energy, and is hence state dependent, and, in general, many body in nature. In the low-concentration limit, (3) reduces to a sum of effective pair interactions between two isolated polymer coils:

$$v_2(|\vec{R}_1 - \vec{R}_2|) = -k_B T \ln[C \times P_2(\vec{R}_1, \vec{R}_2)]. \tag{4}$$

Since global properties of polymeric systems are independent of chemical detail in the scaling $(L \to \infty)$ limit, we adopt henceforth a simple lattice model of polymer solutions, namely that of mutually and self-avoiding walks (SAWs) of length $L = M - 1$ on a cubic lattice of lattice spacing b (equal to the segment length); non-connected nearest-neighbour monomers of the same or different polymer coils have an attractive energy $-\epsilon$. This model accounts for the key polymer features, namely connectivity, excluded volume and solvent quality (through the value of ϵ).

Convenient thermodynamic variables are the polymer density $\rho = N/(\Omega b^3)$ (Ω being the size of the lattice), the monomer density $c = M\rho$ (equivalently the monomer packing fraction $\phi = cb^3$ equal to the number of lattice sites occupied by monomers) and the temperature T ($\beta^* = \epsilon/k_B T$). A key characteristic is the overlap density $\rho^* = 3/4\pi R_g^3$ (where R_g is the radius of gyration, $\sim bL^\nu$) which corresponds to the cross-over from the dilute ($\rho < \rho^*$) to the semi-dilute regimes ($\rho > \rho^*$). The semi-dilute regime differs from the melt in that the monomer packing fraction remains negligible; for any given ρ/ρ^* this is only achieved for sufficiently long polymers, since $\phi = (\rho/\rho^*)L^{(1-3\nu)} \sim L^{-4/5}$ for SAW polymers.

2. Polymers in good solvent

Consider first the athermal limit of SAW polymers ($\epsilon = 0$). In the low ($\rho \to 0$) density limit $P_2(\vec{R}_1, \vec{R}_2)$ is then simply the probability that there is no monomer–monomer overlap for a fixed distance $r = |\vec{R}_1 - \vec{R}_2|$ between the CMs. This is well adapted to Monte Carlo (MC) sampling. Scaling theory predicts that the resulting effective interaction at full overlap, $v_2(r = 0)$, is independent of chain length L [2]. Early simulations with rather short chains pointed to $v_2(r = 0) \approx 2k_B T$ [3]. An in-depth investigation of the L-dependence shows that $v_2(r)$ is well represented by a Gaussian $v_2(r) \approx u \exp(-\alpha(r/R_g)^2)$, where α is of order 1, while $u/k_B T \approx 1.80$ [4, 5].

At finite polymer concentration ρ, three- and more-body effective interactions come into play [6]. A more efficient strategy is to determine an effective density-dependent pair potential $v_2(r; \rho)$ by inverting the CM–CM pair distribution $g(r)$ from full monomer-level MC simulations [6, 7]. It was proven that this inverse problem has a unique solution [8]. The inversion procedure is implemented using the HNC-integral equation [9]. The Ornstein–Zernike relation [9] allows the extraction of the direct correlation function $c(r)$ from the MC data for $h(r) = g(r) - 1$ at any given density. The HNC closure then expresses $v_2(r)$ as [9]

$$\beta v_2(r) = -\ln[g(r)] + h(r) - c(r). \tag{5}$$

The first term on the rhs is the potential of mean force, while $h(r) - c(r)$ describes the effect of correlations.

The MC-generated $g(r)$ show that correlations *decrease* as ρ increases, contrary to the more familiar behaviour observed for hard-core systems. The overlap value $g(r = 0)$ increases steadily towards 1 (the ideal gas value), confirming that in the high-density limit of a melt, polymer chains indeed behave as non-interacting polymers [10]. The resulting effective pair potential is only moderately density dependent and is well fitted by a sum of Gaussians. The range of $v_2(r)$ tends to increase with ρ, and the potential develops a small amplitude

negative tail for r significantly larger than R_g [4, 11]. The link with thermodynamics is via the compressibility relation [9], which allows the osmotic pressure P to be expressed as

$$\beta P(\rho) = \int_0^\rho [1 - \rho' \hat{c}(k = 0; \rho')] \, d\rho' \qquad (6)$$

where $\hat{c}(k)$ is the Fourier transform of $c(r)$. Use of the effective pair potential in conjunction with the virial and energy equations is meaningless [12]. The equations of state calculated from MC simulations of the full monomer level polymer representation and from simulations based on the much less CPU-intensive effective potential representation agree within numerical uncertainties, underlining the adequacy of the HNC inversion procedure for such 'soft' effective particles. Well into the semi-dilute regime ($\rho \gg \rho^*$) the slopes of the calculated equation of state agree with the des Cloizeaux scaling prediction $\beta P \approx \rho^{3\nu/(3\nu-1)} \approx \rho^{9/4}$, where $\nu = 0.588 \approx 3/5$ is the Flory exponent for the radius of gyration in good solvent ($R_g \sim bL^\nu$) [10].

Neglecting the density dependence of $v_2(r)$, i.e. extending the low-density Gaussian form to all densities, brings us back to the 'Gaussian core model' (GCM) first introduced by Stillinger [13], which exhibits interesting behaviour at low temperatures ($\beta^* \gg 1$) [14]. In the regime relevant for polymer solutions ($\beta^* \approx 1$) the model leads to 'mean field fluid' behaviour at sufficiently high density, where the random phase approximation, $c(r) = -\beta v_2(r)$, leads to a quadratic equation of state for $\rho \gg \rho^*$ [14, 15]:

$$\beta P = \rho + \tfrac{1}{2} \beta \hat{v}_2(k = 0) \rho^2. \qquad (7)$$

Incorporating the ρ-dependence of v_2 is found from simulation to change the asymptotic ρ^2 behaviour into des Cloizeaux scaling $\rho^{9/4}$. As a by-product of the GCM, we have developed a multiple occupancy lattice model, which also gives rise to interesting microphase separation [16].

3. From good to poor solvent conditions

We now turn our attention to the case where adjacent monomers attract, i.e. $\epsilon \neq 0$ or $\beta^* > 0$. This attraction is solvent induced, and the quality of the solvent deteriorates as β^* increases, leading to contraction of the polymer coils. At the θ temperature ($\beta_\theta^* = \epsilon/k_B T_\theta$), repulsion and attraction between polymers cancel, at least in the low-density limit, so the polymers exhibit the scaling behaviour of ideal polymers ($R_g \sim L^{1/2}$). Below T_θ, polymer coils collapse into globules ($R_g \sim L^{1/3}$), and phase separation occurs into polymer-rich and polymer-poor solutions.

The most convenient diagnostic for locating T_θ from simulations is to calculate the second virial coefficient $B_2(L; T)$ as a function of temperature and polymer length. The L-dependent Boyle temperature $T_B(L)$ is that at which $B_2(L; T)$ vanishes for a fixed L, then:

$$T_\theta = \lim_{L \to \infty} T_B(L). \qquad (8)$$

This leads to the estimate $\beta_\theta^* = 0.2690 \pm 0.0002$ [17]. Note that $B_2(L; T)$ can be directly expressed in terms of the low-density limit of the effective CM pair potential:

$$B_2(L; T) = 2\pi \int_0^\infty [1 - e^{-\beta v_2(r, L, T)}] r^2 \, dr. \qquad (9)$$

Extensive MC simulations were used to determine the effective pair potential for fixed length $L = 100$ over a wide range of temperatures ($0 \leqslant \beta^* \leqslant 0.3$) and densities ρ [18]. As β^* increases, $v_2(r = 0)$ decreases and $v_2(r)$ develops an attractive tail for $r > R_g$.

Eventually $v_2(r)$ violates Ruelle's necessary condition for the existence of a thermodynamic limit, namely [19]

$$I_2 = \int v_2(r) \, d\vec{r} > 0. \tag{10}$$

Since v_2 depends on L, ρ and T, so does I_2, and for any given ρ and L, the limit of stability temperature T_s is determined by

$$I_2(L, \rho, T = T_s) = 0. \tag{11}$$

Below T_s, single polymer coils will collapse and we conjecture that $T_\theta = \lim_{\rho \to 0} \lim_{L \to \infty} T_s(\rho, L)$ [18]. However, if ρ is increased at a given temperature $T \leqslant T_\theta$ the effective pair potential increasingly reverts to being repulsive until the Ruelle criterion [9] is satisfied, and the polymer solution becomes thermodynamically stable again. This 'restabilization' reflects a phase separation scenario under poor solvent conditions ($T < T_\theta$).

The variation of $v_2(r)$ with temperature and density, as extracted from the HNC inversion of MC data, is semi-quantitatively reproduced by solutions of the PRISM integral equation [20] for the thread model ($b \to 0$, $L \to \infty$ at fixed R_g) of polymer solutions [21, 22]. PRISM assumes all monomers to be equivalent (i.e. neglects end effects) and yields the monomer pair distribution function $g_{mm}(r)$ of a polymer solution. The CM distribution function $g(r)$ required to extract the effective pair potential $v_2(r)$ may be related to $g_{mm}(r)$ by an approximate, but accurate, relation involving internal form factors of a single coil [23]. Further progress along these lines might eventually bypass the need for time-consuming simulations of full monomer level models required to determine $g(r)$.

The equation of state may be computed as a function of ρ/ρ^* and β^*, using a somewhat cumbersome method based on the contact theorem [24, 25], or much more efficiently by subjecting the polymers to a gravitational field and invoking hydrostatic equilibrium [26]. If $\rho(z)$ denotes the CM (or monomer) density profile of the polymers in a vertical field, which is easily measured in simulations, the osmotic pressure at an altitude z is simply

$$\beta P(z) = \frac{1}{\zeta} \int_z^\infty \rho(z') \, dz' \tag{12}$$

where $\zeta = k_B T / Mg$ is the gravitational length, which must be chosen (by tuning the product Mg) significantly larger than R_g for the macroscopic description (which follows from the local density approximation within density functional theory of inhomogeneous fluids) to hold [27]. Elimination of the altitude z between $P(z)$ and $\rho(z)$ then leads to the bulk equation of state $P(\rho)$. Examples from simulations of $L = 500$ chains are shown for four temperatures in figure 1.

4. Long polymers: corrections to scaling

Polymers are critical objects in the universality class of the zero-component ($n = 0$) limit of the *n*-vector model of critical phenomena [28]. The $L \to \infty$ limit is equivalent to the limit of divergent correlation length ξ at the critical point of a second-order phase transition. The properties of very long chains can hence be investigated using the powerful method of the renormalization group (RG) and field theory [29]. These predict two scaling regimes, an athermal one corresponding to the good solvent (SAW) limit, and the second corresponding to the θ-solvent regime where ideal polymer statistics hold. The cross-over between the two regimes is discontinuous in the scaling limit $L \to \infty$. The objective is to predict the behaviour for large but finite L from a finite-size scaling analysis of MC data [30, 5]. We restrict the
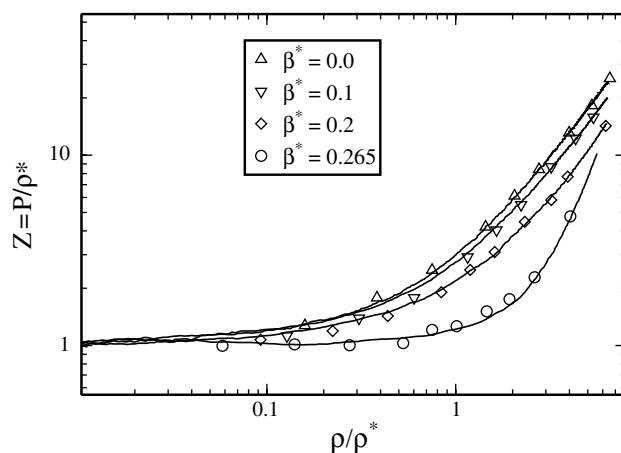
Figure 1. Equation of state on a log–log scale, calculated using Dickman's (contact theorem) method, (symbols) and hydrostatic equilibrium (solid lines).

discussion to the good solvent regime. For $\beta < \beta_\theta$ any universal (dimensionless) ratio R may be represented as

$$R(L, \beta) = R^* + \frac{a_R(\beta)}{L^\Delta} + \cdots \tag{13}$$

where R^* is the temperature-independent scaling limit ($L \to \infty$) and the exponent $\Delta = 0.517$ [31]. Higher-order terms involve exponents of the order of 1 or larger. The temperature-dependent coefficient $a_R(\beta)$ is non-universal, but ratios of such coefficients for two different dimensionless qualities are again universal, i.e. model independent. A much-studied example of a universal ratio is $A_2(L, \beta) = B_2(L, \beta)/R_g^3(L, \beta)$. A similar ratio involving the third virial coefficient $A_3(L, \beta) = B_3(L, \beta)/R_g^6(L, \beta)$ has been examined in detail in [5]. B_3 is found to be always positive, but to go through a sharp minimum near $T = T_\theta$. The effective pair potential between the CMs of two isolated polymers ($\rho \ll \rho^*$ limit), divided by $k_B T$, is another universal ratio, which has been investigated by a similar scaling analysis in [5]:

$$\beta v_2(r, L, \beta) = v_\infty(x) + \frac{a_v(\beta)}{L^\Delta} v_c(x) + \cdots \tag{14}$$

where $x = r/R_g$. v_∞, v_c and $a_v(\beta)$ are extracted from a careful analysis of MC data for several lengths L and inverse temperatures $0 \leqslant \beta < \beta_\theta$. These may then be used to predict βv_2 for any length and temperature, and agreement with MC data is excellent for $\beta^* \leqslant 0.2$ and $L \geqslant 500$. Closer to the θ-temperature the convergence of (14) with L is found, not surprisingly, to be much slower, and one must then switch to the scaling analysis appropriate for the θ-regime. The scaling analysis has been recently extended to binary mixtures of polymers of different lengths and to star polymers [32].

5. Soft polymers and hard colloids

Mixtures of colloidal particles and non-adsorbing polymers have attracted considerable experimental and theoretical attention over the last two decades, because of interesting phase behaviour induced by the familiar depletion mechanism [33]. The effective depletion interaction between spherical colloidal particles may be tuned by varying the size ration $q = R_g/R_c$ (where R_c is the colloid radius), and the polymer concentration ρ. Consider

first the case of polymers between two plates ($q = 0$) separated by z. The depletion potential per unit area $W(z)$ is defined by the difference in polymer grand potentials:

$$W(z) = \frac{1}{A}[\Omega(z) - \Omega(z = \infty)] \tag{15}$$

$$= \int_z^\infty [P(z') - P(z = \infty)]\,\mathrm{d}z'. \tag{16}$$

Clearly since at contact two depletion zones are destroyed $W(z = \infty) = -2\gamma_W(\rho)$, where γ_W is the polymer–wall surface tension. The simple ansatz:

$$W(z) = W(0) + P(\rho)z; \qquad z < D_W(\rho) = -\frac{W(0)}{P(\rho)} \tag{17}$$

$$= 0; \qquad z > D_W(\rho) \tag{18}$$

reproduces direct simulation data well. The result for SAW polymers [34] differs considerably from that for ideal polymers [33]: the range D_W is shorter for interacting polymers, and decreases with increasing density, while it is independent of density for ideal polymers; the contact value $W(0)$ decreases faster with ρ for interacting polymers since the surface tension scales as $\rho^{3/2}$ in the semi-dilute regime [35], while it scales as ρ for ideal polymers. For finite $q \leqslant 1$, the depletion force between two spheres can be approximately related to the depletion potential between two planes via the Derjaguin approximation, and by correcting for the decreasing range of the force due to partial wrapping of the polymer coils around the spherical colloid [34].

Such pair depletion interactions do not, however, account for effective many-body interactions due to finite colloid concentrations. To that purpose the coarse-graining strategy described in sections 1–3 may be extended to the two-component colloid–polymer system. An effective state-dependent colloid–polymer pair interaction $v_{cp}(r)$ may be extracted by an HNC inversion of the polymer density profile around a sphere [4, 11, 34], similar to the inversion procedure used to determine the effective polymer–polymer pair potential $v_{pp}(r)$. The colloid–colloid pair potential $v_{cc}(r)$ is well approximated by a simple hard-sphere interaction. MC simulations of this effective two-component system were used to calculate the phase diagram of the mixture for $q \leqslant 1$ [36]. The calculated binodal agrees very well with experimental data [38] for interacting polymers. Significant qualitative differences arise between phase diagrams for ideal [37] and interacting polymers, particularly for larger q: the range of the concentrated ('liquid') colloidal phase in the colloid density–polymer density plane is considerably reduced when polymer interactions are included, and the critical point occurs at significantly higher packing fraction of the two species [36]. These trends become more pronounced in the 'protein limit' of large polymers and small colloids ($q \gg 1$) [39]. Solvent quality has a strong influence on the induced depletion interaction between colloids, with polymers under θ conditions leading, not surprisingly, to a pair interaction close (but not identical) to that induced by ideal polymers [25], at least for $\rho/\rho^* < 1$.

6. Diblock copolymers and beyond

The coarse-graining strategy may be extended to polymers other than the linear homopolymers considered so far. Star polymers, for instance, have been investigated along similar lines [40]; the CM is replaced by the midpoint where the f arms of a star polymer meet; the resulting effective pair interaction diverges logarithmically as $r \to 0$ and hardens as f increases. The case of symmetric diblock copolymers AB has been examined very recently [41]. The A and B strands are represented as soft 'blobs', the CMs of which are tethered by an 'entropic
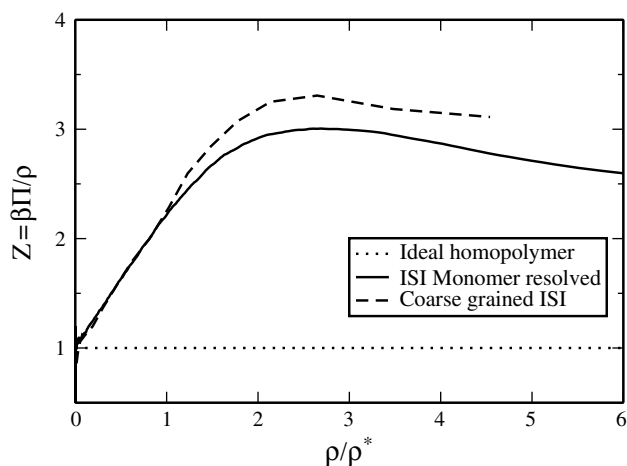
Figure 2. Equation of state generated from MC simulations for diblock copolymers using full monomer level and coarse-grained 'blob' models.

spring' characterized by the intramolecular potential $\phi_{AB}(r)$ which is derived from the MC-generated distribution function of relative distances of the A and B CMs on the same copolymer. There are now three intermolecular CM potentials $v_{AA}(r)$, $v_{BB}(r)$, $v_{AB}(r)$, in addition to the intramolecular potential. The inversion procedure to go from the partial distribution functions $g_{\alpha\beta}(r)$ to the pair potentials $v_{\alpha\beta}(r)$ is now more involved [41]. Even in the low-density limit one already faces a four-body problem. The inversion procedure has been carried out in that limit for a simple athermal model, the ISI model, where A–A and B–B pairs behave like ideal polymers, i.e. freely interpenetrate, while A–B pairs behave like mutually avoiding walks. This is the block copolymer equivalent of the familiar Widom–Rowlinson model [42] which drives phase separation of simple atomic fluids (where A and B are untethered). Because the two strands of the AB block copolymer system are tethered, macroscopic phase separation due to A–B incompatibility is suppressed and reduces to microphase separation: the symmetric block copolymers form a lamellar phase, which was indeed observed in MC simulations of both the full monomeric and the coarse-grained representations [41]. The resulting equation of state calculated by the hydrostatic equilibrium method is shown in figure 2. $Z = \beta P/\rho$ is seen to first increase linearly up to $\rho/\rho^* \approx 2$, where it flattens out, and thereafter decreases slowly to give an asymptotic value > 1. This may be understood by noting that, in the lamellar phase (which develops for $\rho/\rho^* > 2$), the repulsive A–B contacts are greatly reduced. Figure 2 also shows the equation of state calculated (with much less computational effort) for the coarse-grained 'soft-dumbbell' model with effective intra- and inter-molecular pair potentials $\phi_{AB}(r)$ and $v_{\alpha\beta}(r)$ determined in the zero-density limit. The agreement is excellent up to $\rho \approx \rho^*$, and remains semi-quantitative thereafter, despite the fact that the density dependence of the effective potential has not been taken into account.

The 'soft dumbbell' representation of diblock copolymers provides a hint of how to extend the coarse-graining strategy of linear homo or hetropolymers over a wide range of polymer concentrations. As the ratio ρ/ρ^* increases, the fundamental length scale gradually crosses over from R_g (for $\rho/\rho^* < 1$) to the correlation length $\xi \sim \rho^{-3/4}$ deep in the semi-dilute regime, to the segment length b in the melt. The coarse-graining strategy put forward in this paper applies to dilute and initial semi-dilute regimes, where polymer coils are well represented by a single 'soft-core' particle with a radius of the order R_g. Deeper into the semi-dilute regime, the

blob picture [43] applies for polymers confined by other polymers or in a pore; each polymer reduces to a 'necklace' of blobs of radius ξ, tethered by entropic springs; different blobs on the same or neighbouring chains interact via a quasi-Gaussian soft-core potential, as introduced in earlier sections. The radius of each blob decreases, and hence their number increases (for a given overall length L) as the ratio ρ/ρ^* increases, until the melt regime is reached where the blob size reduces essentially to the segment length b, and the coarse-graining strategy is no longer of any use. Over the whole semi-dilute regime a polymer may thus be pictured as a necklace of blobs, and the present coarse-graining strategy allows, in principle, for an unequivocal determination of intra- and inter-molecular effective interactions between these blobs. Work along these lines is in progress.

Acknowledgments

References

[1] Flory P J and Krigbaum W R 1950 *J. Chem. Phys.* **18** 1086
[2] Grosberg A V, Khalatur P G and Khokhlov A R 1982 *Macromol. Chem. Rapid Commun.* **3** 709
[3] Dautenhahn J and Hall C K 1994 *Macromolecules* **27** 5399
[4] Bolhuis P G, Louis A A, Hansen J-P and Meijer E J 2001 *J. Chem. Phys.* **114** 4296
[5] Pelissetto A and Hansen J-P 2005 *J. Chem. Phys.* **112** 134904
[6] Bolhuis P G, Louis A A and Hansen J-P 2001 *Phys. Rev.* E **64** 021801
[7] Louis A A, Bolhuis P G, Hansen J-P and Meijer E J 2000 *Phys. Rev. Lett.* **85** 2522
[8] Henderson R L 1974 *Phys. Lett.* A **49** 197
[9] Hansen J-P and McDonald I R 1986 *Theory of Simple Liquids* 2nd edn (London: Academic)
[10] see e.g. Rubinstein M and Colby R H 2003 *Polymer Physics* (Oxford: Oxford University Press)
[11] Bolhuis P G and Louis A A 2002 *Macromolecules* **35** 1860
[12] Louis A A 2002 *J. Phys.: Condens. Matter* **14** 9187
[13] Stillinger F H 1976 *J. Chem. Phys.* **65** 3968
[14] Lang A, Likos C N, Watzlawek M and Löwen H 2000 *J. Phys.: Condens. Matter* **12** 5087
[15] Louis A A, Bolhuis P G and Hansen J-P 2000 *Phys. Rev.* E **62** 7961
[16] Finken R, Hansen J-P and Louis A A 2004 *J. Phys. A: Math. Gen.* **37** 577
[17] Grassberger P and Hegger R 1995 *J. Chem. Phys.* **102** 6881
[18] Krakoviack V, Hansen J-P and Louis A A 2003 *Phys. Rev.* E **67** 041801
[19] Ruelle D 1969 *Statistical Mechanics: Rigorous Results* (London: Benjamin)
[20] For a review see Schweizer K S and Curro J G 1997 *Adv. Chem. Phys.* **97** 1
[21] Fuchs M and Schweizer K S 2001 *Phys. Rev.* E **64** 021514
[22] Krakoviack V, Rotenberg B and Hansen J-P 2004 *J. Phys. Chem.* B **108** 6697
[23] Krakoviack V, Hansen J-P and Louis A A 2002 *Europhys. Lett.* **58** 53
[24] Dickman R 1987 *J. Chem. Phys.* **87** 2246
[25] Addison C I, Louis A A and Hansen J-P 2004 *J. Chem. Phys.* **121** 612
[26] Addison C I, Hansen J-P and Louis A A 2005 *Chem. Phys. Chem.* **6** 1760
[27] Barrat J-L, Biben T and Hansen J-P 1995 *J. Chem. Phys.* **102** 6881
[28] de Gennes P G 1972 *Phys. Lett.* A **38** 339
[29] See, e.g., Freed K F 1987 *Renormalization Group Theory of Macromolecules* (New York: Wiley)
[30] Li B, Madras N and Sokal A D 1995 *J. Stat. Phys.* **80** 661
[31] Belohorec P and Nickel B 1997 *Guelph University Report* unpublished
[32] Pelissetto A 2005 private communication
[33] Asakura S and Oosawa F 1954 *J. Chem. Phys.* **22** 1255
[34] Louis A A, Bolhuis P G, Meijer E J and Hansen J-P 2002 *J. Chem. Phys.* **117** 1893

[35] Louis A A, Bolhuis P G, Meijer E J and Hansen J-P 2002 *J. Chem. Phys.* **116** 10547
[36] Bolhuis P G, Louis A A and Hansen J-P 2002 *Phys. Rev. Lett.* **89** 128302
[37] Lekkerkerker H N W *et al* 1992 *Europhys. Lett.* **20** 559
      Meijer E J and Frenkel D 1994 *J. Chem. Phys.* **100** 6873
[38] Ramakrishnan S, Fuchs M, Schweizer K S and Zukoski C F 2002 *J. Chem. Phys.* **116** 2201
[39] Bolhuis P G, Meijer E J and Louis A A 2003 *Phys. Rev. Lett.* **90** 068304
[40] For a review, see Likos C N 2001 *Phys. Rep.* **348** 267
[41] Addison C I, Hansen J-P, Krakoviack V and Louis A A 2005 *Mol. Phys.* **103** 3045
[42] Widom B and Rowlinson J S 1970 *J. Chem. Phys.* **52** 1670
[43] de Gennes P G 1979 *Scaling Concepts in Polymer Physics* (Ithaca, NY: Cornell University Press)